American Journal of Biomedical Engineering 2013, 3(4): 91-98
DOI: 10.5923/j.ajbe.20130304.02

Computational Analysis of Catheter-Tip Geometries for Optimizing Drug Infusion in Arterial Blood Flow

Kiyya Ararsa , Ralph C. Aldredge

Department of Mechanical and Aerospace Engineering, University of California, Davis, CA, 95616, USA

Abstract Intra-arterial infusion therapy is an effective treatment of localized malignant diseases. This type oftherapy reduces systemic toxicity and enhances tumor response. However, poor mixing and non-uniform drug dispersion can lead to a buildup of toxic local concentrations and thereby decrease the effectiveness of the therapy. In this study, we investigate the mixing properties of six catheters with varying tip geometries to address the problem of local toxicity. Using a 3D, turbulent, incompressible, two-fluid, unsteady formulation, the goal of the study is to qualitatively compare and determine which catheter-tip geometries produce the most optimal mixing characteristics distal to the catheter tip and deliver the highest drug concentration to the vessel walls. The open-source code OpenFOAM is used to model blood and drug flow dynamics. Our resultsshow that modified catheters with side holes exhibitthe best spreading and mixing properties andthat lower-viscositydrug solutions are more effective than higher-viscosity drug solutionsat the same injection flow rates.

Keywords Catheter Design, Drug Infusion Therapy, Bio-fluid Dynamics, Blood-flow Modeling, OpenFOAM

1. Introduction

The practice of intra-arterial infusion of drugs for the treatment of localized malignant diseases has been longstanding in the field of interventional radiology[1, 2]. The objective of this therapy is to deliver an appropriate drug concentration locallyto the infused region, with a lowered drug concentration in systemic circulation. However, local toxicity is a common problem associated with intra-arterial infusion techniques[1]. One of the more probable causes of local toxicity is insufficient mixing of the drug solution with blood at the point of infusion, associated with non-uniform streaming from the catheter tip, as shown by Lutz and Miller[3]. Lutz *et al*.[4] proposed increasing thedrug-solution infusion rate to combat the local toxicity problem. Unfortunately, higher infusion rates have several drawbacks; for example, (a) possible jesting, whipping and recoiling of the catheter on the vascular wall and (b) higher injection pressures that may be difficult to maintain with some catheter-tip designs and with high-viscosity drug solutions. Higher drug-infusion rates are also impractical in chronic medical treatments, as they result in larger volumes of ingestedfluid[5-7]. Ultimately, effective intra-arterial drug-infusion therapy requires adequate local spreading and mixing in the vicinity of the catheter tip.

* Corresponding author:
rcaldredge@ucdavis.edu (Ralph C. Aldredge)
Published online at http://journal.sapub.org/ajbe

Several studies have been conducted on catheter tip geometries to enhance local spreading and mixing properties. Weber *et al*.[8] investigated the addition of side holes and slits to a standard peripheral end-hole catheter. Their 1D inviscidstudy concluded that the addition of side holes and slits results in the drug solution having a pattern less like a jet streamand more like a plume, better mixing with the blood flow andlower shear stress at the blood-vessel wall.

Mongrain *et al*.[9] conducted a 2D, steady numerical simulation of the performance of four catheter-tip geometries (*standard end hole, vortex, flush and cloud*) in a straight arterial vessel using commercial CFD software, FLUENT. The results of their study, which employeda steady, 2D viscous generalisation of the ID non-viscous approach presented in Hansen *et al*.[10], were found to agree qualitatively with experimental observations. However, the authors noted the limitations of their model in addressing the inherently unsteady, 3D nature of the flow. In particular, the steady, 2D model cannot account for the influence of turbulence transport, which can appreciably influence the extent of local mixing of an infused drug solution with the surrounding blow flow.

In thepresent study, we investigate the mixing properties of six different catheters using an incompressible 3D, two-fluid, unsteady numerical formulation that fully accounts for turbulence effects. In addition, we consider two additional catheter-tip geometries (toposcopic and modified flush), not considered by Mongrain *et al*.[9]. Ournumerical simulations are conducted using OpenFOAM [11]open-source CFD software with an incompressible

Navier-Stokes solver for two miscible fluids (basedan Eulerian volume-fraction approach) andthe realizable k-εturbulence model.

The objective of our work is to qualitatively compare catheter-tip geometriesto determine which will produce the most optimal mixing characteristics distal to the catheter tip. The study also investigates the effects of viscosity by comparing the performance of two different infused solutions. A radiographic contrast material (Iopamidol 370) and a saline solution were chosen based on their relative viscosities and densities relative to those of blood[12]. Both laminar andturbulent flowsare considered in order to examine the effects of turbulent mixing. The two injection flow ratesthat we consider are 1 ml/s &21 ml/s for the contrast material and 1 ml/s &2.1 ml/s for saline solution. The flow rate of theblood is kept constant throughout ourstudy at 5.9 ml/s, so that the arterial blood-flow speed and Reynolds number in the region upstream from the catheter tip are 26.8 cm/s and 421, respectively, consistent with the laminar flow regime.

2. Formulation

Certain assumptions were made to simplify the complexity of blood flow dynamics, considering the challenges associated with modeling blood flow[13]. For example, the rheology of blood flow is generally non-Newtonian due to the presence of diverse elements, includingred and white blood cells and plasma; as blood is a living tissue, the components of which areinfluenced by chemical and electrical signals in the body. Furthermore, the blood flow is pulsatile and the blood vessels are viscoelastic, both ofwhich can create a highly unsteady flow field[14]. As in Mongrain *et al*. [9], the blood and the injected solutions are both modeled as incompressible and Newtonian, because of the high shear rates (greater than 100/s) in the vicinity of the catheter jet where velocity gradients are large), and the rigid-wall assumption ismade. The pulsatile behavior of the blood flow is neglected also, consistent with the fact thatthe time period of interest is only a fraction of theheart-cycle period; the time for complete mixing and spreading of the injected solution over the computational domainis less than 0.1 seconds for all cases considered. However, our formulation fully accounts for the transient behavior of the blood and catheter-fluid flows,especially important near the tip of the catheter where the effects of turbulent mixing are most relevant.

The governing equations describing hemodynamics in a blood vessel are derived from principles of mass, momentum, and energy conservation. A volume-fraction transport equation is used to characterize the mixing of blood with the injected solution. The volume fraction of blood, denoted α_1, is defined as0 (1) in regions where there is only drug solution (blood) and between 0 and 1 elsewhere where there is a mixture of blood and the injecteddrug solution. The volume fraction of the injected solution α_2 is determined from $\alpha_2 = 1 - \alpha_1$ once α_1 is known. The mass-continuity and momentum equations are formulated to take into account the material and interfacial properties of the fluids.

The governing equations for the volume fraction α_1, mean flow velocity $\bar{\mathbf{u}}$ and pressure p aregiven below. In these equations, $v_f \equiv D + \mu_t / \rho Sc_t$, where μ_t is the turbulence viscosity ,Sc_t is the turbulence Schmidt number and D is the mass diffusivity of the injected drug solution in blood, equal to 10^{-9} m^2/s for saline and twice as large for the contrast solution. The mixture density is defined by $\rho \equiv \alpha_1\rho_1 + \alpha_2\rho_2$ and the effective viscosity by $\mu_{eff} \equiv \mu + \mu_t$, with the mixture molecular viscosity given by $\mu \equiv \alpha_1\mu_1 + \alpha_2\mu_2$. In Eq. (1), $\bar{\mathbf{u}}$ is the ensemble-averaged mixture-flow velocity.

$$\left.\begin{aligned} \nabla\cdot\bar{\mathbf{u}} &= \mathbf{0} \\ \frac{\partial\alpha_1}{\partial t} + \bar{\mathbf{u}}\cdot\nabla\alpha_1 &= \nabla\cdot\left(v_f\nabla\alpha_1\right) \\ \frac{\partial}{\partial t}\left(\rho\bar{\mathbf{u}}\right) + \nabla\cdot\left(\rho\bar{\mathbf{u}}\bar{\mathbf{u}}\right) &= -\nabla p + \left[\nabla\cdot\left(\mu_{eff}\nabla\right)\right]\bar{\mathbf{u}} \end{aligned}\right\} \quad (1)$$

The turbulence model employed in our simulations for calculation of the turbulence viscosity μ_t is the realizable k-ε model, based on the Reynolds-Averaged Navier-Stokes (RANS) equations. This model was chosen over the standard k-ε model because it is more accurate at predicting the spreading rate of both planar and rounds jets, and it was concluded from a qualitative assessment of turbulence models that better accuracy of flow behavior can be achieved with the realizable k-ε model at low Reynolds numbers. The governing equations of the model are as follows[15].

$$\frac{\partial}{\partial t}\left(\rho k\right) + \nabla\cdot\left(\rho k\mathbf{u}\right) = \nabla\cdot\left[\left(\mu + \mu_t k/\sigma_k\right)\nabla k\right] + \mu_t S^2 - \rho\varepsilon \quad (2)$$

$$\begin{aligned} \frac{\partial}{\partial t}\left(\rho\varepsilon\right) + \nabla\cdot\left(\rho\varepsilon\mathbf{u}\right) = \nabla\cdot\left[\left(\mu + \mu_t k/\sigma_\varepsilon\right)\nabla\varepsilon\right] \\ + C_1 S\rho\varepsilon - C_2\rho\varepsilon^2/\left(k + \sqrt{\nu\varepsilon}\right) \end{aligned} \quad (3)$$

where,

$$S = \sqrt{S_{ij}S_{ij}}, \quad S_{ij} = \frac{1}{2}\left(\frac{\partial\bar{u}_j}{\partial x_i} + \frac{\partial\bar{u}_i}{\partial x_j}\right), \quad \Omega_{ij} = \left(\frac{\partial u_i}{\partial x_j} - \frac{\partial u_j}{\partial x_i}\right) \quad (4)$$

and

$$\left.\begin{aligned} C_\mu &= \left[4.04 + \sqrt{6}\cos(\phi)kU^*/\varepsilon\right]^{-1}, \ \phi = \cos^{-1}\left(\sqrt{6}W\right)/3 \\ U^* &= \sqrt{S_{ij}S_{ij} + \Omega_{ij}\Omega_{ij}}, \ W = S_{ij}S_{jk}S_{ki}/S \\ C_1 &= \max\left(0.43, \eta/(\eta+5)\right), \ \eta = Sk/\varepsilon \\ C_2 &= 1.9, \ \sigma_k = 1.0, \ \sigma_\varepsilon = 1.2 \\ k &= \sqrt{\tfrac{1}{2}\left\langle(\mathbf{u}-\bar{\mathbf{u}})\cdot(\mathbf{u}-\bar{\mathbf{u}})\right\rangle}, \ \mu_t = C_\mu\rho k^2/\varepsilon \end{aligned}\right\} \quad (5)$$

3. Computational Model

3.1. Catheter Geometry

The dimensions of thecomputational domain are similar to those ofMongrain *et al*. [9], but with a few modifications. The inner diameters of the blood vessel and catheter are 5.5 mm and 1mm, respectively, while the length of the computational domain (theblood-vessel length) is 70 mm. The computational domain encompasses the regions inside and outside of the final 30 mm of the catheter as well as the various openings in the catheter tip, as shown in Fig. 1.

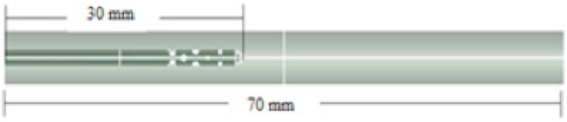

Figure 1a. Cloud Catheter (side view)

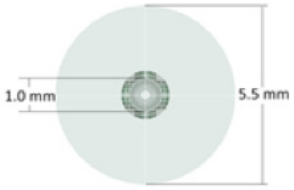

Figure 1b. Cloud Catheter (axial view)

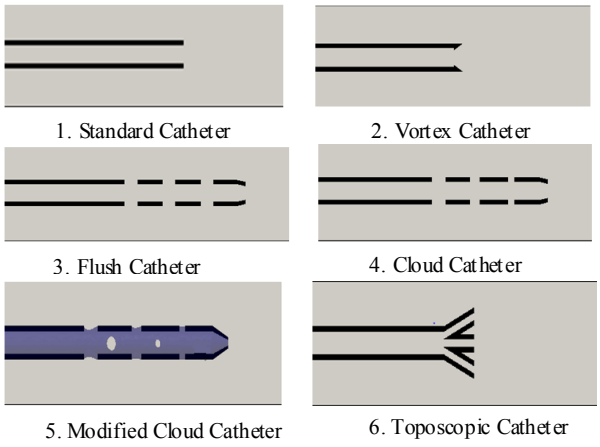

Figure 2. Catheter-tip geometries (not to scale)

Figure 2 shows the various catheter-tip geometries considered. The catheters all have the same wall thickness of 0.25 mm. The inner diameter (ID) of each catheter upstream from the tip is 1 mm, which is also ID of the standard end-hole catheter at its tip. Theend hole of the vortex [16], flush and cloud catheters are all tapered to 0.79 mm ID, while the modified-cloud catheter has an end-hole ID of 0.25 mm. All side holes in the flush catheter have a diameter of 0.79 mm. The cloud catheter, however, has side holes of increasingly smaller diameter(0.89, 0.64 and 0.38 mm) with decreasing distance from the catheter tip, as proposed by Hansen *et al*.[10] to equalize the flow rate out of the side holes. With the exception of the modified cloud catheter, each catheter has a total of six holes. In these, there are two identical diametrically opposed side holes centered in each of three radial cross sections, the first located 3 mm from the catheter tip and the others separated 3 mm apart along the catheter axis.

The modified-cloud catheter has a total of ten side holes, six of which are identical in size and location to those of the cloud catheter, laid out as described above. Its other four side holes are laid out in two additional, secondary planes separated 3 mm apart, one of which is located 4.5 mm from the catheter tip. Each of these secondary planes has two identical diametrically opposed side holes that are offset 90 degrees along the circumference relative to the locations of the side holes in the primary planes, as shown in Fig. 2. The side holes in the secondary plane located 4.5 mm from the catheter tip have a diameter of 0.38 mm while the other two (located in the plane 7.5 mm upstream of the catheter tip) have a diameter of 0.64 mm.

3.2. Numerical Methods

A finite-volume method (FVM) was used to solve Eqs. (1)-(5) using open-sourcecode provided in OpenFoam 2.10 [11], a collection of C++ libraries. Specifically, the solver twoLiquidMixingFoam was used, with a second-order implicit backward scheme (upwind)for discretization oftime (convection) derivatives. The other spatial gradients were discretized via second-order Gauss integration. The simulation was conducted for a total of 0.1 seconds with the timesteps being controlled by aCFL of 0.75, based on the smallest grid spacing (0.05 mm) and themaximum velocity amplitude found for each time step. The computation was accomplished on a cluster of 16 - 20 processor nodes. Our computational grid is defined by a 3D unstructured tetrahedral mesh, created with SALOME 6.5. Table 1 summarizes the characteristics of the meshemployed for eachtype ofcatheter.

Table 1. Mesh Characteristics

Geometry	Type	# of Points	# of Cells
Standard	tetrahedral	44,717	184,192
Vortex	tetrahedral	113,002	468,051
Flush	tetrahedral	44,707	183,377
Cloud	tetrahedral	45,034	185,396
Modified Cloud	tetrahedral	68,149	281,328
Toposcopic	tetrahedral	44,468	180,485

The catheter is assumed to be stationary and concentrically oriented, in the middle of the blood vessel. The velocities at the catheter and blood-vessel inlet locations, at the left edge of the computational domain, are steady and parabolic, consistent with annular Poiseuille flow. No-slip boundary conditions are applied at the blood-vessel wall and turbulent wall functions are employed near the wall. At the blood-vessel outlet, a zero-gradient or outflow condition is imposed. Because the simulation is incompressible, only the pressure gradient is relevant, and therefore the outlet pressure is set to a reference value of zero. The boundary conditions are summarized in Table 2; and thermodynamic and transport properties of the blood and of the saline and contrast infusion fluids are summarized in Table 3.

Table 2. Summary of Boundary Conditions

Geometry	Blood volume Fraction (α_1)	Velocity (U)	Pressure (p)	Turbulence Kinetic Energy (k)	Turbulence Dissipation (ϵ)
Blood at Inlet	1	Flow Rate	Zero Gradient	Intensity	Mixing Length
Drug at Inlet	0	Flow Rate	Zero Gradient	Intensity	Mixing Length
Outlet	Zero Gradient	Zero Gradient	Fixed Value = 0	Inlet/Outlet	Inlet/Outlet
Catheter at Wall	Zero Gradient	No Slip	Zero Gradient	Wall Function	Wall Function
Blood at Wall	Zero Gradient	No Slip	Zero Gradient	Wall Function	Wall Function

Table 3. Summary of Physical Properties

Name	Fluid Type	Density (kg/m^3)	Viscosity (cP)	Mass Diffusivity (m^2/s)	S_{c_t}
Blood	Human	1170	3.5	--	1.42
Contrast Material	Iopromide 370	1410	21	2.00E-09	
Saline Solution	Hypertonic Saline 3%	1007	1.5	1.00E-09	

4. Results

4.1. Blood Volume-Fraction Iso-contours

Figure 3 compares the distribution of blood volume fraction in the blood vesselaround each ofthe six catheter types at a time of 0.7 seconds, representing the attainment of steady state, for saline-solution injection into the blood vessel at the rate of 1 ml/s. Values of the iso-contoursrange from 0, for pure saline, to 1 for pure blood, with intermediary values representing a mixture of the two fluids. Our results compare well qualitatively with the those of Mongrain *et al.* [9] but provide greater detail of the flow field. For example, the differences between the cloud and flush catheters are more evident in our results, where it can be seen that the flow exiting the third hole (farthest away) from the tip of the flush catheter has a lower flow rate than that from the same hole of the cloud catheter.

The standard, vortex and toposcopic catheters exhibit poor spreading of the infused saline solution to the vessel wall when compared to the flush, cloud and modified cloud catheters. The standard and vortex catheters inducea streaming of the infused substance. Contrary to the design objective, the vortex catheter does not create mixing in the vicinity of the tip, nor does it create vortex sheading. However, it does result is enhanced diffusion of the injected solution into the blood flow, in comparison with that of the standard catheter design. The toposcopic catheter creates a low-pressure region in the vicinity of the tip, which draws the flow coming out of the side holes towards the middle of the blood vessel and away from the walls.Thus, downstream of the toposcopic-catheter tip the flow is very similar to that of the vortex catheter. It is obvious from Fig. 3 that the best performing catheters are the flush, cloud and modified cloud catheters, with performance measured by how fast the injected drug solution reaches the vessel walls, having mixed thoroughly with the surrounding blood flow. For a quantitative measure this performance, the spreading rates of the various catheters are compared in Figs. 4-7.

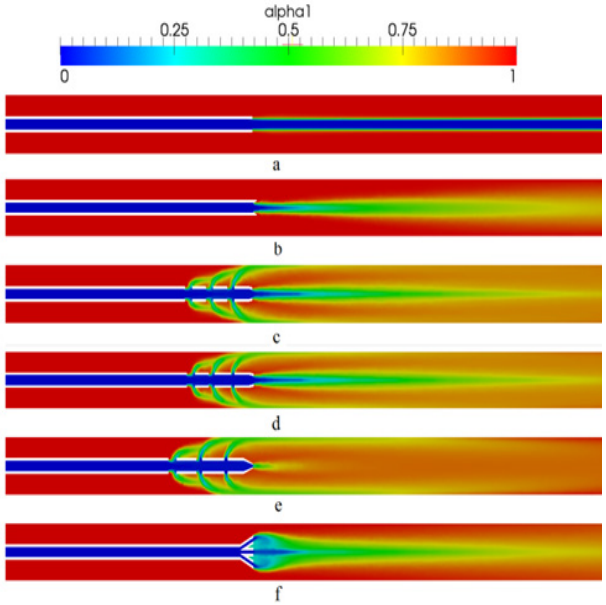

Figure 3. Iso-contours of blood-volume fraction at a simulation time of 0.7s, for saline-solution injection of 1ml/s; for four catheter types: (a) Standard, (b) Vortex, (c) Flush, (d) Cloud, (e) Modified Cloud, (f) Toposcopic

4.2. Spreading & Mixing

To assess the spreading efficiency of the catheters, the blood volume fraction α_1 is plotted against the radialdistance from the catheter centerline at various locations downstream of the catheter tip. Figs. 4-7 show thevolume fraction at locations 1mm, 5mm, 10mm and 20mm downstream of the catheter tip for saline-solution injection at the rate of 1 ml/s. All measurements were taken in the same computational symmetry planeas that illustrated in Fig. 3. Optimal results should show small, nearly constant α_1 across the blood-vessel cross-section.

Figure 4 illustrates the spreading of saline solution injected into the blood vessel at a location 1 mm downstream of the catheter tip. At this location the blood volume fraction α_1 is either negligible or small at the centerline ($r = 0$) for all

but the modified-cloud catheter geometry, for which the volume fraction of the injected saline solution $(1-\alpha_1)$ has been reduced to 20% as a result of substantial mixing at the centerline. However, the saline volume fraction drops off substantially as the blood-vessel wall is approached for all of the catheter types considered. Saline solution reaches the blood-vessel wall (with a volume fraction of about 40%) only for the catheters with side holes. Of these, the modified-cloud catheter performs best, with the most substantial mixing and dilution of the blood over the selected blood-vessel cross section. As exhibited in Figs. 5-7, the superior performance of the modified cloud catheter in this regard is even more distinct at locations farther downstream from the catheter tip.

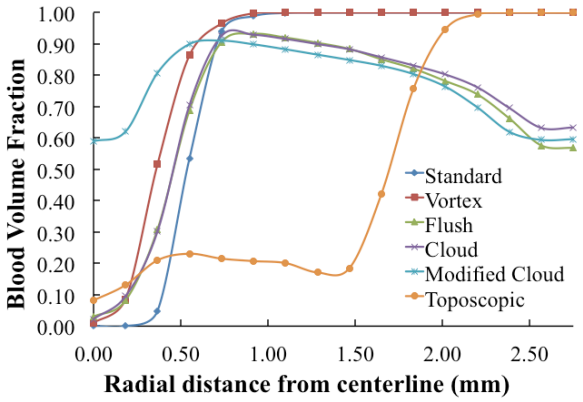

Figure 4. Volume fraction of bloodα_1 plotted versus radial distance from the catheter centerline, at a distance 1 mm downstream of catheter tip

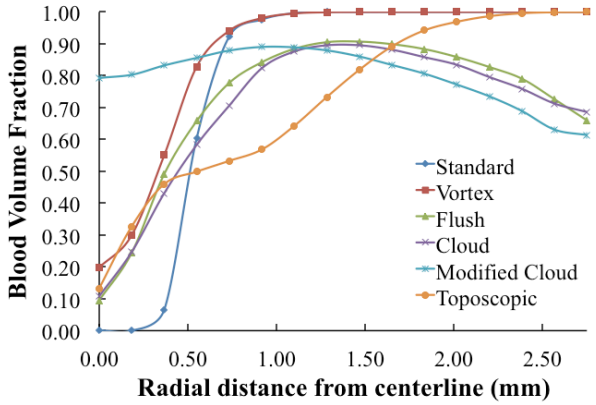

Figure 5. Volume fraction of blood α_1 plotted versus radial distance from the catheter centerline, at a distance5 mm downstreamof catheter tip

In general, the flow rate of saline solution out of the tip of the catheters with side holes is relatively small. This is due to the fact that the majority of saline solution exits the side holes, so that not much is left to exit from the tip opening. This is a favorable result because it reduces the amount of intra-arterial infusion of the catheter fluid and also makes extravasation of the blood-vessel wall less likely to occur.

4.3. Turbulence Effects

To investigate the influence of injection flow rate on the spreading rate of the infused fluid, we considered three different injection flow rates, characterizing laminar, transition, and turbulent flow within the catheter. These flow rates are 1, 2.1 and 5 ml/s, respectfully. Lutz*et al*. [4] found enhanced mixing of the infused drug solution with blood with increased infusion rate. However, these investigators did not consider catheters with side holes, the performance of which is more sensitive to the injected-fluid flow rate, as demonstrated in the results of our study presented in Figs. 8-10. These plots show saline solution at simulation time of 0.025 s.

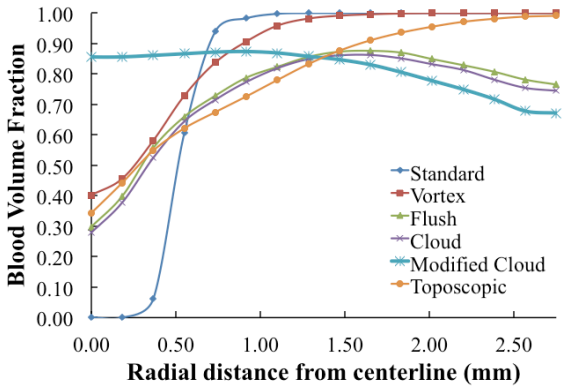

Figure 6. Volume fraction of bloodα_1 plotted versus radial distance from the catheter centerline, at a distance 10 mm downstream of catheter tip

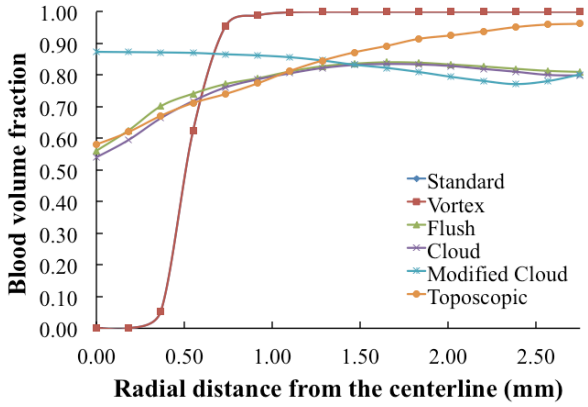

Figure 7. Volume fraction of bloodα_1 plotted versus radial distance from the catheter centerline, at a distance 20 mm downstream of catheter tip

Each figure shows two columns of results, one for each of the six catheter types (as specified in the figure captions). The first (last) row of results in each figure pertains to the lowest (highest) injection flow rate considered, for which flow within the catheter is expected to be laminar (turbulent), based on a Reynolds number of 855 (4274). The middle row pertains to the intermediate injection flow rate of 2.1 ml/s, for which flow within the catheter is expected to be consistent with transitional flow, based on a Reynolds number of 1795.At the simulation time of 0.025 s selected for the snap shots of bloodvolume fraction presented in Figs. 8-10, the flow in blood vessel has not yet attained steady state for the lower saline-solution flow rates. It is clear, however, that he extent of mixing and spreading of the saline

solution throughout the blood vessel significantly increases with increasing injection flow rate, for all of the catheter types considered. The turbulent injected saline solution (for the highest injection flow rate considered) reaches the blood vessel wall much more quickly than in the cases of laminar and transitional injected saline solution.As for the case of laminar injected saline, presented earlier in Figs. 4-7, the modified-cloud catheter performs best among all of the catheter types when the injected saline is transitional or turbulent. It is clear from Figs. 9 and 10, however, that the jets of injected fluid exiting the side holes of the flush, cloud and modified-cloud catheters impinge directlyon the blood-vessel wall, for the highest injection flow rates considered (1 &2.1 ml/s). This can potentially result in excessively large normal and shear stresses on the blood-vessel wall.

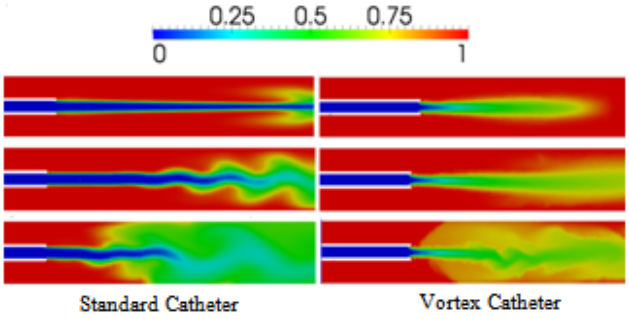

Figure 8. blood volume-fraction plotsfor laminar (top row: Re = 855), transitional (middle: Re = 1795) and turbulent (bottom: Re = 4244) saline-solution flow within the Standard & Vortex catheters

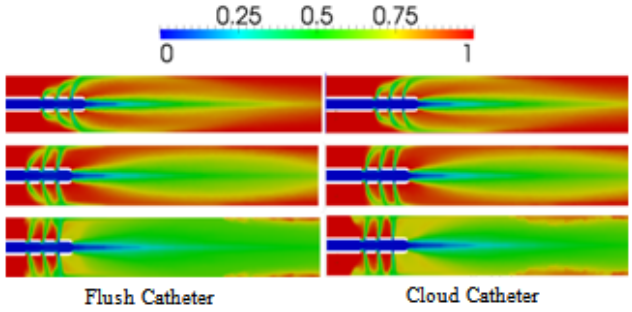

Figure 9. blood volume-fraction plots for laminar (top row: Re = 855), transitional (middle: Re = 1795) and turbulent (bottom: Re = 4244) saline-solution flow within the Flush & Cloud catheters

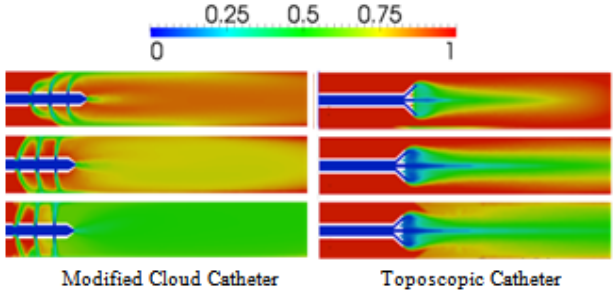

Figure 10. blood volume-fraction plots for laminar (top row: Re = 855), transitional (middle: Re = 1795) and turbulent (bottom: Re = 4274) saline-solution flow within the Modified-Cloud & Toposcopic catheters

4.4. Viscous Effects

To investigate the influence of viscosity on mixing and spreading of a drug infused into the blood vessel, the injection of Iopromide 370 was simulated as a contrast to hypertonic saline solution. The kinematic viscosity of Iopromide 370 is approximately five times that ofblood, while the kinematic viscosity of saline solution is half that of blood (c.f., Table 2). Therefore, in conjunction with the results presented above for saline-solution injection, simulations with Iopromide 370 will allow the comparison of results obtained for a drug solution that is significantly more viscous than the bloodstream flow with those obtained for a drug solution that is significantly less viscous than the bloodstream flow. For these comparisons, we will consider only the flush and vortex catheters (representative of catheters with and without side holes, respectively).

Figure 11 shows a comparison of blood volume fractions predicted for contrast and saline-solution injection at the rate of 1 ml/s from a vortex catheter, at the simulation time of 0.07 s. It is found that the less-viscous saline solution spreads into the blood flow more effectively than the contrast solution (Iopromide 370). This result is consistent with the fact that the Reynolds number for the contrast-solution in the catheter is greater than that for saline, based on the difference in the viscosities of the two fluids. Figure 12 shows a comparison of blood volume fractions predicted for contrast and saline-solution injection at the rate of 1 ml/s from a flush catheter, at the simulation time of 0.03 s.In this case there is little difference between the spreading effectiveness of the two injected fluids downstream of the catheter tip, although the concentration of the injected fluid is significantly higher at the blood vessel wall upstream of the catheter tip, near the side holes, when the contrast solution is used. This is a consequence ofthe influence of the dynamic pressure of the blood flowing past the catheter side holes, which causes more stream-wise deflection of the less-viscous saline solution.

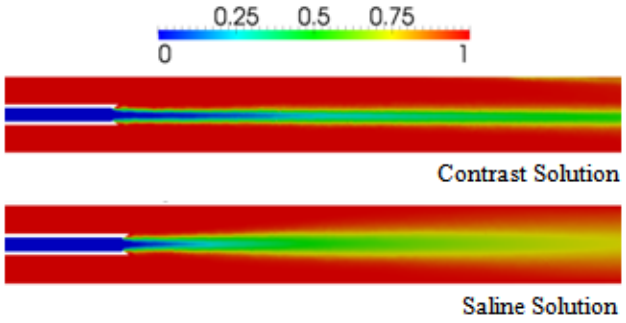

Figure 11. Comparison of blood volume fractions predicted for contrast and saline-solution injection at the rate of 1 ml/s from a vortex catheter, at a time of 0.07s

As a result, a larger amount of the more viscous contrast solution makes it from the side holes to the blood-vessel wall upstream of the catheter tip, relative to that of the saline solution. This in turn results a lower flow rate of contrast solution out of the catheter tip, in comparison with that of the saline solution, as can be seen in Fig. 12. Therefore, it can be

concluded that higher-viscosity fluids are better suited for catheters that take advantages of side holes.

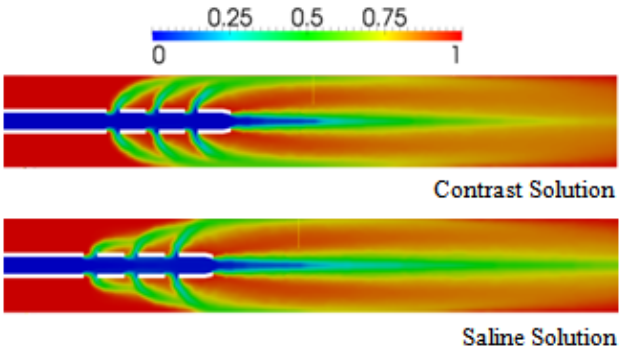

Figure 12. Comparison of blood volume fractions predicted for contrast and saline-solution injection at the rate of 1 ml/s from a flush catheter, at a time of 0.03 s

Figure 13 provides a comparison of blood volume fractions predicted for contrast and saline-solution injection at the rate of 5 ml/s from a vortex catheter, at a simulation time of 0.03 s. The saline (contrast) solution in the catheter is predicted to be turbulent (laminar), with Re = 4274 (408). However, the characters of the simulated flows downstream of the catheter appear to be very similar.This is likely due to the complex dynamics of the shear layer initially separating the injected-fluid and blood flows at the exit of the catheter, which may be significantly more unstable when the viscosity of the injected fluid is much higher than that of the blood (as is the case for the contrast fluid).

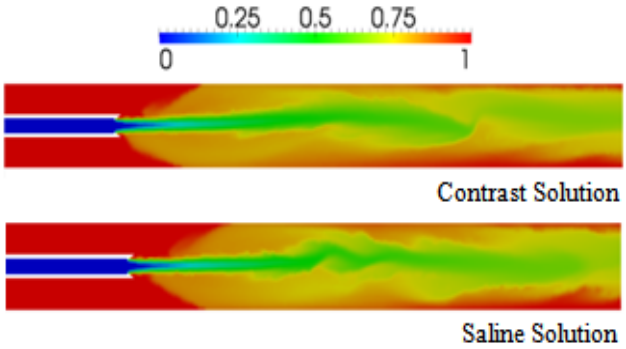

Figure 13. Comparison of blood volume fractions predicted for contrast and saline-solution injection at the rate of 5 ml/s from a vortex catheter, at a time of 0.03 s

Figure 14 shows a comparison of blood volume fractions predicted for saline-solution (contrast-solution) injection at the rate of 2.1 (21) ml/s from a vortex catheter, at a simulation time of 0.03 s. Both the saline and contrast solutions are predicted to be transitional at these flow rates, with Re = 1795 and 1714, respectively. The jet of contrast solutionvery quickly becomes turbulent downstream of the catheter tip, while the jet of saline solution appears to remain laminar through the entire computational domain. Consequently, mixing and spreading of the contrast solution occurs much more effectively than that of the saline solution.This again illustrates the importance of the ratio of the catheter-fluid viscosity to that of the blood flow as a separate parameter, independent of the Reynolds number, that influences mixing and spreading effectiveness.

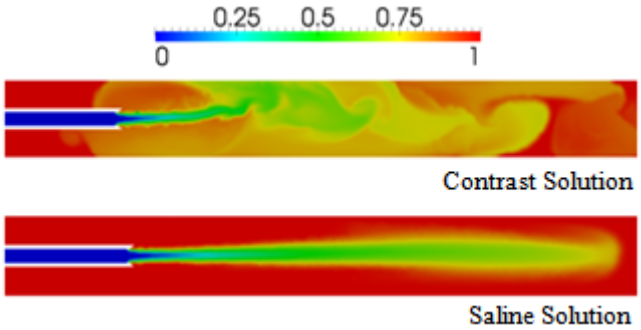

Figure 14. Comparison of blood volume fractions predicted for saline (contrast) injection at the rate of 2.1 (21) ml/s from a vortex catheter, at a time of 0.03 s

5. Conclusions

In this study, we have investigated the mixing and spreading effectiveness of several catheter-tip geometries and the influence ofinjection-fluid viscosity, flow rateand turbulence transport. We employed an incompressible 3D, two-fluid, unsteady numerical formulation that fully accounts for turbulence effects using the realizable k-εturbulence model. The results of our simulations improve on the 2D results of Mongrain et al.[12] by providing a more detailed characterization of the dynamics of theinteraction between theinjected drug solutionand the blood flow. This greater detail allows ultimately for a determination of which catheter geometries provide the most effective spreading of the injected drug solution toward the blood-vessel wall and mixing of the injected drug solution with the blood.

The vortex catheter was found to enhance mixing and spreading of the injected fluid beyond that of the standard catheter design. The toposcopic catheter is characterized bya low pressure near its tip that, which is associated with recirculation of the flow back toward the blood-vessel centerline. This type of catheter also provides enhanced mixing and spreading of the injected fluid over that of the standard catheter design. The addition of holes in the catheter wall, near its tip, was found to further enhance spreading andmixing, due to the direction of injected-fluid momentum directly toward the blood-vessel wall.Of the catheter designs with side holes considered, the modified cloud catheter (with additional, circumferentially staggered side holes of varying diameter) was found to provide the most effective spreading and mixing of the injected fluid for given injection-fluid flow rate and viscosity.

6. Discussion

If the flow rateis too high, then a drug solution injected into the blood stream from a catheter with side holes may damage the blood-vessel wall. In fact, a higher risk of

infection is found with the use of catheters with side holes for hemodialysis, in comparison with that found with catheters without side holes[17]. Not with standing this, side-hole catheters are the most efficient at spreading an injected drug solution to an area of interest within the blood vessel,for appropriate injection rates.

In general, the spreading effectiveness of a catheter is ultimately determined by the flow rate of the injected fluidand is greatest at large flow rates. In addition, spreading and mixing with the surrounding bloodmay be substantially enhanced by turbulence transport. The viscosity of the injected fluid is important in determiningits flow rate, which is inversely proportional to the fluid viscosity, and whether or not it is turbulent. For a given pressure drop supplied across the catheter from inlet to exit, the flow rate within the catheter will be greatest with a low-viscosity fluid, which is also more likely than a higher-viscosity fluid to be turbulent within the catheter. However, the results of our simulations show also that the jet of injected fluid emanating from the catheter may be turbulent when the ratio of the injected-fluid viscosity is substantially larger than the viscosity ofblood, even when the fluid is laminar within the catheter.

Finally, it should be noted that as blood-flow dynamics are inherently unsteady, future workshould consider time-dependent injection profiles and pulsating-blood flow, as well as non-Newtonian constitutive relations for blood.

ACKNOWLEDGEMENTS

We are grateful for access to computational clusters provided by Professor Roger Davis at UC Davis.

REFERENCES

[1] H. Chen, and J. Gross, “Intra-arterial infusion of anticancer drugs: theoretic aspects of drug delivery and review of responses,” *Cancer treatment reports,* vol. 64, no. 1, pp. 31, 1980.

[2] J. Y. Cheong, K. M. Lee, S. W. Cho, J. H. Won, J. K. Kim, H. J. Wang, K. B. Hahm, and J. H. Kim, “Survival benefits of intra-arterial infusion chemotherapy in patients with advanced hepatocellular carcinoma with portal vein tumor thrombosis,” *Hepatology research,* vol. 32, no. 2, pp. 127-133, 2005.

[3] R. J. Lutz, and D. L. Miller, “Mixing studies during hepatic artery infusion in an in vitro model,” *Cancer,* vol. 62, no. 6, pp. 1066-1073, 1988.

[4] R. J. Lutz, R. L. Dedrick, J. W. Boretos, E. H. Oldfield, J. B. Blacklock, and J. L. Doppman, “Mixing studies during intracarotid artery infusions in an in vitro model,” *Journal of neurosurgery,* vol. 64, no. 2, pp. 277-283, 1986.

[5] K. H. BARTH, R. J. LUTZ, P. W. KREMERS, and D. L. MILLER, “Mixing Problems of Low Flow Hepatic Artery Infusion Improvement with Small Caliber Double Lumen Balloon Catheters,” *Investigative Radiology,* vol. 23, no. 7, pp. 519, 1988.

[6] J. Bec, H. Xie, D. Yankelevich, F. Zhou, Y. Sun, N. Ghata, R. Aldredge, and L. Marcu, "Design, construction, and validation of a multimodal intravascular diagnostic catheter combining IVUS and fluorescence lifetime spectroscopy detection channels." p. 788337.

[7] J. Froelich, K. H. Barth, R. J. Lutz, S. V. Lossef, and D. Lindisch, “Injection Characteristics and Downstream Contrast Material Distribution of Flush Aortography Catheters: In Vitro Study,” *Journal of Vascular and Interventional Radiology,* vol. 3, no. 4, pp. 713-718, 1992.

[8] P. W. Weber, C. A. Coursey, L. E. Howle, R. C. Nelson, E. B. Nichols, and S. T. Schindera, “Modifying peripheral IV catheters with side holes and side slits results in favorable changes in fluid dynamic properties during the injection of iodinated contrast material,” *American Journal of Roentgenology,* vol. 193, no. 4, pp. 970-977, 2009.

[9] R. Mongrain, K. Kandarpa, A. Garon, O. Bertrand, and M. Bertrand, “Study of catheter designs and drug mixing processes using 2D steady numerical simulations,” *Medical and Biological Engineering and Computing,* vol. 37, no. 1, pp. 64-70, 1999.

[10] E. Hansen, M. Hawkins, I. Hawkins, E. Akins, S. Miles, and J. Collela, “New high-flow" cloud" catheter for safer delivery of contrast material,” *Radiology,* vol. 173, no. 2, pp. 461-464, 1989.

[11] "The OpenFOAM® Foundation,"http://www.openfoam.org.

[12] "RxList: The Internet Drug List," http://www.rxlist.com/ultravist-drug.htm.

[13] S. Canic, J. Tambaca, G. Guidoboni, A. Mikelic, C. J. Hartley, and D. Rosenstrauch, “Modeling viscoelastic behavior of arterial walls and their interaction with pulsatile blood flow,” *SIAM Journal on Applied Mathematics,* vol. 67, no. 1, pp. 164-193, 2006.

[14] R. L. Fournier, *Basic transport phenomena in biomedical engineering*: CRC Press, 2011.

[15] T.-H. Shih, J. Zhu, and J. L. Lumley, “A realizable Reynolds stress algebraic equation model,” 1993.

[16] J. Shanebrook, K. Tillotson, and B. Weick, “Vortex mixing catheter,” *Medical and Biological Engineering and Computing,* vol. 30, no. 1, pp. 123-124, 1992.

[17] J. Cheesbrough, R. Finch, and R. Burden, “A prospective study of the mechanisms of infection associated with hemodialysis catheters,” *Journal of Infectious Diseases,* vol. 154, no. 4, pp. 579-589, 1986.